

# Tensor $A_{yy}$ and vector $A_y$ analyzing powers in the $H(d, d')X$ and $^{12}C(d, d')X$ reactions at initial deuteron momenta of 9 GeV/ $c$ in the region of baryonic resonances excitation.

V.P. Ladygin\*, L.S. Azhgirey, S.V. Afanasiev, V.V. Arkhipov, V.K. Bondarev, Yu.T. Borzounov, L.B. Golovanov, A.Yu. Isupov, V.I. Ivanov, A.A. Kartamyshev, V.A. Kashirin, A.N. Khrenov, V.I. Kolesnikov, V.A. Kuznetsov, N.B. Ladygina, A.G. Litvinenko, S.G. Reznikov, P.A. Rukoyatkin, A.Yu. Semenov, I.A. Semenova, G.D. Stoletov, A.P. Tzvinev, V.N. Zhmyrov, L.S. Zolin  
*Joint Institute for Nuclear Research, Dubna, Russia*

G. Filipov<sup>†</sup>

*Institute of Nuclear Research and Nuclear Energy, Sofia, Bulgaria*

(Dated: October 16, 2018)

The angular dependence of the tensor  $A_{yy}$  and vector  $A_y$  analyzing powers in the inelastic scattering of deuterons with a momentum of 9.0 GeV/ $c$  on hydrogen and carbon have been measured. The range of measurements corresponds to the baryonic resonance excitation with masses  $\sim 2.2$ – $2.6$  GeV/ $c^2$ . The  $A_{yy}$  data being in good agreement with the previous results demonstrate an approximate  $t$  scaling up to  $-1.5$  (GeV/ $c$ )<sup>2</sup>. The large values of  $A_y$  show a significant role of the spin-dependent part of the elementary amplitude of the  $NN \rightarrow NN^*$  reaction. The results of the experiment are compared with model predictions of the plane-wave impulse approximation.

PACS numbers: 24.70.+s, 25.10.+s, 25.70.Ef

## I. INTRODUCTION

Inelastic scattering of polarized deuterons on hydrogen and nuclei at high energies has been investigated during the last decade in Dubna [1]–[5] and Saclay [6, 7]. The main goal of these studies is to investigate the properties of the baryonic resonances via measurements of polarization observables in the  $(d, d')X$  reaction.

Since the deuteron is an isoscalar probe, inelastic scattering of deuterons on hydrogen,  $H(d, d')X$ , is selective to the isospin 1/2 and can be used to obtain information on the formation of baryonic resonances  $N^*(1440)$ ,  $N^*(1520)$ ,  $N^*(1680)$ , and others. The measurements of analyzing powers, polarizations of the scattered deuterons and different polarization transfers could allow one to obtain the spin-flip probabilities of the  $(d, d')$  reaction sensitive to the quantum numbers of baryonic resonances. The set of observables for the reconstruction of the spin-flip probabilities in the  $A(d, d')A^*$  has been proposed in ref.[8]. Such an experiment has been realized at RIKEN [9] at 270 MeV to study the excitation levels of  $^{12}C$ .

At the same time, inelastic scattering of deuterons on nuclei at high transferred momenta can be considered as a complementary method to elastic  $pd$ - and  $ed$ -scattering, deuteron breakup reaction, electro- and photodisintegration of the deuteron to investigate the deuteron spin structure at short distances and to search for the manifestation of non-nucleonic degrees of freedom.

However, due to lack of the experimental techniques to measure the polarization of the high-energy deuterons, only tensor and vector analyzing powers in the  $(d, d')X$  reaction have been obtained in the vicinity of the baryonic resonances excitation.

The tensor analyzing power  $T_{20}$  in the vicinity of the Roper resonance ( $P_{11}(1440)$ ) excitation has been measured on hydrogen and carbon targets at Dubna [1] and on hydrogen target at Saclay [6]. The measurements of  $T_{20}$  in the deuteron scattering at 9 GeV/ $c$  on hydrogen and carbon have been performed for missing masses up to  $M_X \sim 2.2$  GeV/ $c^2$  [2]. The experiments have shown a large negative value of  $T_{20}$  at momentum transfers of  $t \sim -0.3$  (GeV/ $c$ )<sup>2</sup>. Such a behaviour of the tensor analyzing power has been interpreted in the framework of the  $\omega$ -meson exchange model [10] as due to the longitudinal isoscalar form factor of the Roper resonance excitation and deuteron form factors  $t$ -dependences [11]. The measurements of the tensor and vector analyzing powers  $A_{yy}$  and  $A_y$  at 9 GeV/ $c$  and 85 mrad of the secondary deuterons emission angle in the vicinity of the undetected system mass of  $M_X \sim 2.2$  GeV/ $c^2$  [3] have shown large values. The obtained results are in satisfactory agreement with the plane wave impulse approximation (PWIA) calculations [12]. It was pointed out that the spin-dependent part of the  $NN \rightarrow NN^*$  ( $\sim 2.2$  GeV/ $c^2$ ) amplitude is significant. Recent measurements of the tensor  $A_{yy}$  and vector  $A_y$  analyzing powers in the vicinity of the excitation of baryonic resonances with masses up to  $\sim 1.8$  GeV/ $c^2$  [4, 5] demonstrated large spin effects and the sensitivity to the baryonic resonances properties. The exclusive measurements in the  $H(d, d')X$  reaction in the vicinity of the Roper resonance excitation performed recently at Saclay [7] have also shown large values of the

\*Electronic address: ladygin@sunhe.jinr.ru

<sup>†</sup>Also at Joint Institute for Nuclear Research, Dubna, Russia

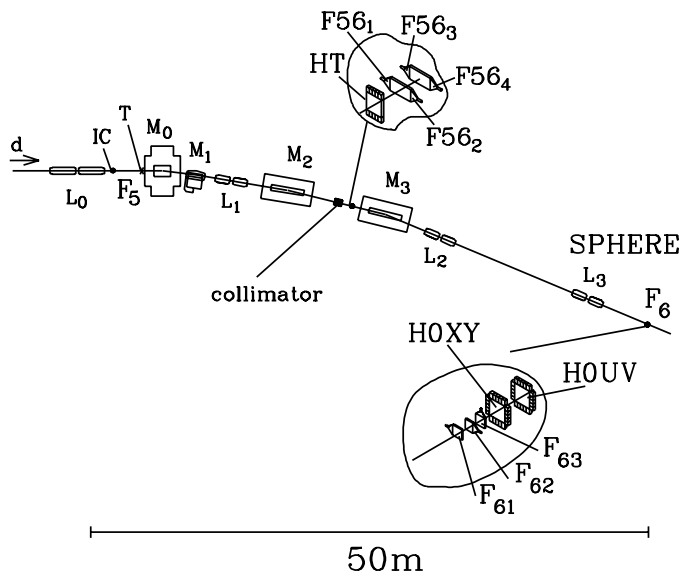


FIG. 1: Schematic view of the experiment.  $M_i$  and  $L_i$  are the magnets and quadrupole lenses doublets, respectively;  $IC$  is an ionization chamber;  $T$  is a target;  $F_{61}$ ,  $F_{62}$ ,  $F_{63}$  are trigger counters;  $F_{561-4}$  are scintillation counters and  $HT$  is a scintillation hodoscope for TOF measurements;  $HOXY$  and  $HOUV$  are beam profile hodoscopes.

$A_{yy}$  and  $A_y$  analyzing powers.

In this paper we report new results on the tensor and vector analyzing powers  $A_{yy}$  and  $A_y$  in deuteron inelastic scattering on hydrogen and carbon at the incident deuteron momentum of 9.0 GeV/c and missing masses of undetected system of  $\sim 2.0$ – $2.6$  GeV/c<sup>2</sup>. Details of the experiment are described in Section II. The comparison with existing data and theoretical predictions is given in Section III. Conclusions are drawn in Section IV.

## II. EXPERIMENTAL PROCEDURE

The experiment has been performed using the polarized deuteron beam at the Dubna Synchrophasotron and the SPHERE setup [3, 4] described elsewhere and shown in Fig.1. The polarized deuterons were produced by the ion source POLARIS [13]. The sign of beam polarization changed cyclically and spill-by-spill: "0", "−", "+", where "0" means the absence of polarization, "+" and "−" correspond to the sign of  $p_{zz}$  with the quantization axis perpendicular to the plane containing the mean beam orbit in the accelerator.

The tensor polarization of the beam was periodically measured during the experiment using the  $A(d, p)X$  reaction at zero emission angle and a proton momentum of  $p_p \sim \frac{2}{3}p_d$  [14], using the same setup. It has been shown that deuteron breakup reaction in those kinematical conditions has very large tensor analyzing power  $T_{20} = -0.82 \pm 0.04$ , independent of the atomic number of the target ( $A > 4$ ) and of the momentum of

the incident deuterons between 2.5 and 9.0 GeV/c [15]. The tensor polarization, corrected for dead time effect [16], and averaged over the whole duration of the experiment was  $p_{zz}^+ = 0.798 \pm 0.002(\text{stat.}) \pm 0.040(\text{syst.})$  and  $p_{zz}^- = -0.803 \pm 0.002(\text{stat.}) \pm 0.040(\text{syst.})$  in "+" and "−" beam spin states, respectively.

The vector polarization of the beam was measured from the asymmetry of quasi-elastic  $pp$ -scattering on a thin CH<sub>2</sub> target placed at focus  $F_4$  about 20 m upstream of the setup [17, 18]. The values of the vector polarization were obtained using the results of asymmetry measurements at a momentum of 4.5 GeV/c per nucleon and 8° proton scattering angle. The corresponding value of the effective analyzing power of the polarimeter  $A(\text{CH}_2)$  amounted  $0.123 \pm 0.006$  [18]. The vector polarization of the beam in different spin states was  $p_z^+ = 0.275 \pm 0.016(\text{stat.}) \pm 0.014(\text{syst.})$  and  $p_z^- = 0.287 \pm 0.016(\text{stat.}) \pm 0.014(\text{syst.})$ , respectively.

A slowly extracted deuteron beam with a typical intensity of  $5 \times 10^8$  to  $10^9$   $\bar{d}$ /spill was directed onto a liquid hydrogen target of 30 cm length or onto carbon targets with different length. The beam intensity was monitored by an ionization chamber placed in front of the target. The beam positions and profiles at certain points along the beam were monitored during each spill. The beam size at the target point was  $\sigma_x \sim 0.4$  cm and  $\sigma_y \sim 0.9$  cm in the horizontal and vertical directions, respectively.

Most of the data were obtained at secondary deuteron emission angles of 85, 130, and 160 mrad and deuteron momenta between 4.5 and 7.0 GeV/c on hydrogen and carbon. The secondary particles emitted from the target were transported to focus  $F_6$  by means of three bending magnets and three quadrupole doublets.

The measurements with empty target were performed at secondary particle momenta of 4.5 and 6.0 GeV/c, while the measurements without target were carried out at 4.5 GeV/c only. The ratio of the yields without target to a 7 cm carbon target was less than  $\sim 1\%$  for the both 85 mrad and 130 mrad detection angle. The yield of particles for empty target was  $\sim 3.5\%$  and  $\sim 11\%$  of the yield from 30 cm liquid hydrogen target at 4.5 and 6.0 GeV/c, respectively, independent of emission angle.

The coincidences of signals from scintillation counters  $F_{61}$ ,  $F_{62}$  and  $F_{63}$  were used as a trigger. Along with the inelastically scattered deuterons, the apparatus detected the protons originating from deuteron fragmentation. The time-of-flight (TOF) information with a base line of  $\sim 34$  m between start counter  $F_{61}$  and stop counters  $F_{561}$ – $F_{562}$ ,  $F_{563}$ – $F_{564}$  and a scintillation hodoscope HT was used for particle identification in the off-line analysis. The TOF resolution was better than 0.2 ns ( $1\sigma$ ). The separation of the particles for different momenta of the detected secondaries is demonstrated in Fig.2. The panels (a), (b), (c), (d), (e) and (f) correspond to secondary particle momenta of 4.5, 5.0, 5.5, 6.0, 6.5, and 7.0 GeV/c, respectively. One can see that the relative contribution of protons becomes more pronounced with decreasing momentum. The residual background

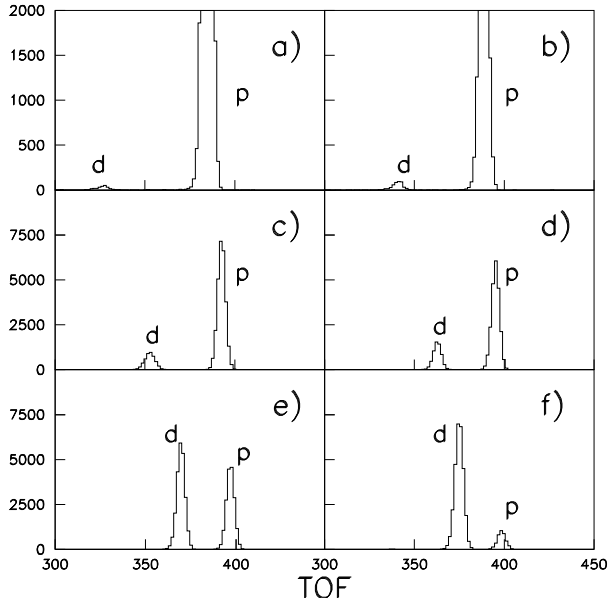


FIG. 2: TOF spectra (in time-to-digit converter channel numbers) obtained for different setting of the magnetic elements. The panels (a), (b), (c), (d), (e), and (f) correspond to secondary particles momenta of 4.5, 5.0, 5.5, 6.0, 6.5, and 7.0 GeV/c, respectively.

was eliminated completely by the requirement that particles are detected at least in two prompt TOF windows.

The acceptance of the setup was determined via Monte Carlo simulations, taking into account the parameters of the incident deuteron beam, nuclear interactions and multiple scattering in the target, in the air, in the windows and detectors, energy losses of primary and secondary deuterons. The momentum and polar angle acceptances were  $\Delta p/p \sim \pm 2\%$  and  $\pm 8$  mrad, respectively.

The missing mass values  $M_X$  were calculated under the assumption that the reaction occurs on a target with proton mass. In this case, the 4-momentum transfer  $t$  and the missing mass  $M_X$  are related as follows

$$M_X^2 = t + m_p^2 + 2m_p Q, \quad (1)$$

where  $m_p$  is the proton mass and  $Q$  is the energy difference between incident and scattered deuteron. The shadowed areas *a*, *b*, and *c* in the kinematic plot given in Fig.3 demonstrate the regions of 4-momentum  $t$  and missing mass  $M_X$  covered by the acceptance setup in the present experiment at detection angle of  $\sim 85$ , 130, and 160 mrad, respectively. The solid line corresponds to an initial deuteron momentum of 9.0 GeV/c and zero emission angle [2]. One can see that the conditions of the present experiment allow one to significantly extend the  $t$  range of measurements for missing masses  $M_X \sim 2.2$ –2.6 GeV/c<sup>2</sup>.

The tensor  $A_{yy}$  and vector  $A_y$  analyzing powers were calculated from the numbers of protons  $n^+$ ,  $n^-$  and  $n^0$ ,

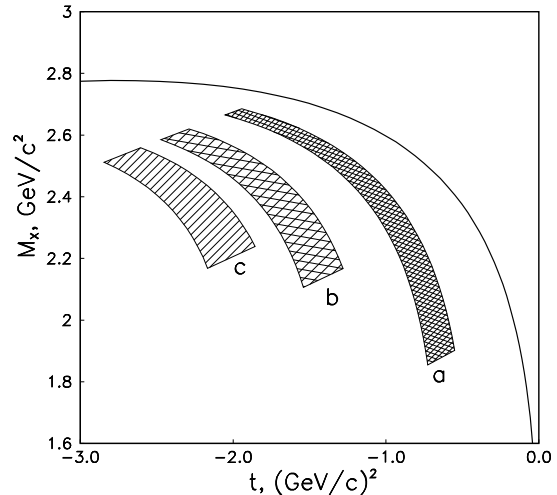


FIG. 3: The kinematical plot of the missing mass  $M_X$  versus 4-momentum  $t$  at the initial deuteron momentum 9.0 GeV/c. The solid line correspond to the conditions (middle of the acceptance) of the experiment performed at zero angle [2]. The shadowed areas *a*, *b*, and *c* demonstrate the regions of 4-momentum  $t$  and missing mass  $M_X$  covered within the acceptance of the present experiment at the deuteron detection angles of  $\sim 85$ ,  $\sim 130$ , and  $\sim 160$  mrad, respectively.

detected for different states of the beam polarization, normalized to the corresponding beam intensities and corrected for the dead time effect [16]. The calculations were carried out by the expressions

$$A_{yy} = 2 \frac{p_z^- (n^+/n^0 - 1) - p_z^+ (n^-/n^0 - 1)}{p_z^- p_{zz}^+ - p_z^+ p_{zz}^-},$$

$$A_y = -\frac{2}{3} \frac{p_{zz}^- (n^+/n^0 - 1) - p_{zz}^+ (n^-/n^0 - 1)}{p_z^- p_{zz}^+ - p_z^+ p_{zz}^-}. \quad (2)$$

These expressions, taking into account different values of polarization in different beam spin states, are simplified significantly when  $p_z^+ = p_z^-$  and  $p_{zz}^+ = -p_{zz}^-$ . The systematic errors due to the uncertainty of the polarization measurements were  $\sim 5\%$  for both the tensor and vector analyzing powers.

### III. RESULTS AND DISCUSSION

The data on  $A_{yy}$  and  $A_y$  with the statistical errors for the  $^1\text{H}(d, d')X$  and  $^{12}\text{C}(d, d')X$  are presented in the Tables I and II, respectively.

The results of the present experiment on the tensor analyzing power  $A_{yy}$  in the  $(d, d')X$  reaction are shown in Fig.4 as a function of the transferred 4-momentum  $t$ . The open circles, triangles and squares are the data obtained on a carbon target at detection angles of  $\sim 85$ ,  $\sim 130$ , and  $\sim 160$  mrad, respectively. The cross and star correspond to the  $A_{yy}$  data for a carbon target taken at  $\sim 115$  and

TABLE I: Results on the tensor  $A_{yy}$  and vector  $A_y$  analyzing powers of the  ${}^1\text{H}(d, d')X$  reaction at initial deuteron momentum 9 GeV/c. ( $\theta$  and  $P$  are the polar angle and momentum of the secondary deuteron, respectively;  $\Delta P$  is momentum acceptance of the setup (FWHM),  $t$  is 4-momentum transfer,  $M_X$  is missing mass.)

$\theta$ , mrad	$P$ , GeV/c	$\Delta P$ , GeV/c	$t$ , (GeV/c) <sup>2</sup>	$M_X$ , GeV/c <sup>2</sup>	$A_{yy} \pm$ $\Delta A_{yy}$	$A_y \pm$ $\Delta A_y$
0.085	4.541	0.095	-1.875	2.651	-0.110 $\pm$ 0.294	0.037 $\pm$ 0.283
0.085	5.041	0.105	-1.466	2.562	-0.013 $\pm$ 0.074	-0.183 $\pm$ 0.196
0.085	6.047	0.125	-0.940	2.302	0.066 $\pm$ 0.065	0.189 $\pm$ 0.062
0.085	6.554	0.137	-0.782	2.132	0.053 $\pm$ 0.041	0.174 $\pm$ 0.039
0.130	4.555	0.096	-2.246	2.575	0.061 $\pm$ 0.247	-0.277 $\pm$ 0.235
0.130	5.051	0.109	-1.883	2.475	0.042 $\pm$ 0.165	-0.092 $\pm$ 0.156
0.130	6.061	0.130	-1.446	2.184	-0.024 $\pm$ 0.047	0.101 $\pm$ 0.045

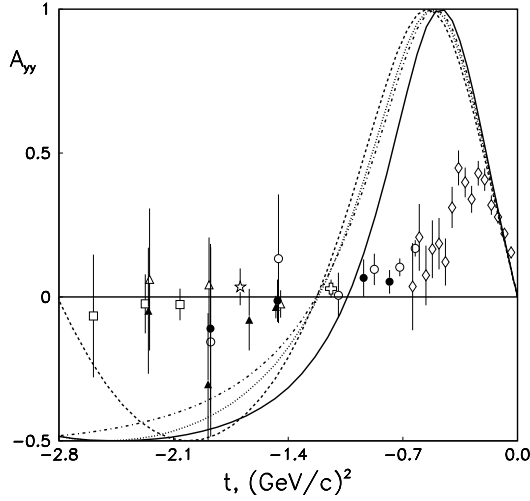


FIG. 4: Tensor analyzing power  $A_{yy}$  in the  $(d, d')X$  reaction obtained at 9 GeV/c. The symbols are explained in the text. The solid, dashed, dotted and dash-dotted lines are predictions in the framework of PWIA [12] using DWFs for Paris [19] and Bonn A, B and C [20] potentials, respectively.

$\sim 145$  mrad. The filled circles and triangles denote the data obtained on a hydrogen target at  $\sim 85$  and  $\sim 130$  mrad, respectively. The data of the present experiment are compared with the data taken at zero angle on hydrogen [2] given by the diamonds. One can see that the values of  $A_{yy}$  obtained at different emission angles are in good agreement demonstrating an approximate  $t$ -scaling observed in earlier experiments [1]-[5]. The present data along with the data from previous experiments allow one to trace the general behaviour of  $A_{yy}$  over a wide region

TABLE II: Results on the tensor  $A_{yy}$  and vector  $A_y$  analyzing powers of the  ${}^{12}\text{C}(d, d')X$  reaction at initial deuteron momentum 9 GeV/c. ( $\theta$  and  $P$  are the polar angle and momentum of the secondary deuteron, respectively;  $\Delta P$  is momentum acceptance of the setup (FWHM),  $t$  is 4-momentum transfer,  $M_X$  is missing mass.)

$\theta$ , mrad	$P$ , GeV/c	$\Delta P$ , GeV/c	$t$ , (GeV/c) <sup>2</sup>	$M_X$ , GeV/c <sup>2</sup>	$A_{yy} \pm$ $\Delta A_{yy}$	$A_y \pm$ $\Delta A_y$
0.085	4.544	0.089	-1.873	2.650	-0.156 $\pm$ 0.329	0.470 $\pm$ 0.314
0.085	5.050	0.098	-1.460	2.559	0.133 $\pm$ 0.224	0.264 $\pm$ 0.213
0.085	5.606	0.105	-1.094	2.429	0.006 $\pm$ 0.079	0.161 $\pm$ 0.075
0.085	6.109	0.116	-0.875	2.285	0.096 $\pm$ 0.054	-0.070 $\pm$ 0.051
0.085	6.616	0.126	-0.719	2.113	0.103 $\pm$ 0.031	0.134 $\pm$ 0.030
0.085	7.117	0.131	-0.625	1.911	0.169 $\pm$ 0.029	0.120 $\pm$ 0.027
0.115	6.587	0.131	-1.138	2.024	0.029 $\pm$ 0.032	0.147 $\pm$ 0.030
0.130	4.563	0.087	-2.254	2.570	-0.048 $\pm$ 0.219	0.100 $\pm$ 0.208
0.130	5.070	0.096	-1.889	2.467	-0.303 $\pm$ 0.247	0.298 $\pm$ 0.235
0.130	5.590	0.107	-1.638	2.321	-0.079 $\pm$ 0.107	0.257 $\pm$ 0.102
0.130	6.094	0.116	-1.476	2.156	-0.035 $\pm$ 0.039	0.023 $\pm$ 0.037
0.145	6.097	0.118	-1.694	2.104	0.035 $\pm$ 0.064	0.087 $\pm$ 0.061
0.160	4.590	0.091	-2.589	2.490	-0.066 $\pm$ 0.214	0.275 $\pm$ 0.204
0.160	5.095	0.097	-2.272	2.373	-0.024 $\pm$ 0.102	0.155 $\pm$ 0.097
0.160	5.600	0.109	-2.060	2.225	-0.026 $\pm$ 0.055	0.044 $\pm$ 0.053

of  $|t|$ . At small  $|t|$  ( $\leq 0.3$  (GeV/c)<sup>2</sup>),  $A_{yy}$  rises linearly up to a value of  $\sim 0.4$ , then it smoothly decreases towards zero at  $|t| \sim 1.0$ – $1.4$  (GeV/c)<sup>2</sup>.

The data obtained on hydrogen and carbon targets are in good agreement. The observed independence of the tensor analyzing power on the atomic number of the target indicates that rescattering in the target and medium effects are small. Hence, nuclear targets are appropriate to obtain information on baryonic excitations in inelastic scattering.

The results on the tensor  $A_{yy}$  and vector  $A_y$  obtained at 9 GeV/c and 85 mrad [4] and at 5 GeV/c and 178 mrad [5] have been satisfactorily explained in the framework of the PWIA approach [12] (see diagram in Fig. 5a). In this model the tensor and vector analyzing powers are expressed in terms of three amplitudes ( $T_{00}$ ,  $T_{11}$  and  $T_{10}$ ) defined by the deuteron structure and the ratio  $r$  of the spin-dependent to spin-independent parts of the elementary process  $NN \rightarrow NN^*$  in the vicinity of  $\sim 2.2$

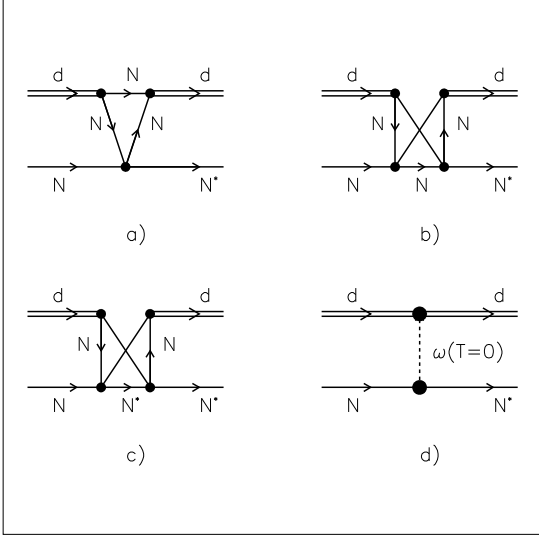


FIG. 5: Diagrams representing mechanisms of baryonic excitation in deuteron–nucleon collisions: (a) plane wave impulse approximation; (b) and (c) double-collision mechanism; (d)  $\omega$ -meson exchange mechanism.

GeV/c<sup>2</sup>:

$$A_{yy}(q) = \frac{T_{00}^2 - T_{11}^2 + 4r^2 T_{10}^2}{T_{00}^2 + 2T_{11}^2 + 4r^2 T_{10}^2}, \quad (3)$$

$$A_y(q) = 2\sqrt{2}r \frac{(T_{11} + T_{00})T_{10}}{T_{00}^2 + 2T_{11}^2 + 4r^2 T_{10}^2}. \quad (4)$$

Amplitudes  $T_{00}$  and  $T_{11}$  depend on the deuteron wave function:

$$\begin{aligned} T_{00} &= S_0(q/2) + \sqrt{2}S_2(q/2), \\ T_{11} &= S_0(q/2) - \frac{1}{\sqrt{2}}S_2(q/2), \end{aligned} \quad (5)$$

where  $S_0$  and  $S_2$  are the spherical and quadrupole form factors of the deuteron expressed in the following manner:

$$\begin{aligned} S_0(q/2) &= \int_0^\infty (u^2(r) + w^2(r))j_0(rq/2)dr, \\ S_2(q/2) &= \int_0^\infty 2w(r) \left( u(r) - \frac{1}{2\sqrt{2}}w(r) \right) j_2(rq/2)d(6) \end{aligned}$$

Here,  $u(r)$  and  $w(r)$  are  $S$ - and  $D$ - waves of the deuteron in coordinate space, respectively,  $j_0(qr/2)$  and  $j_2(qr/2)$  are the Bessel functions of zero and second order, respectively, and  $q^2 = -t$ .

The amplitude  $T_{10}$  is also function of  $S$ - and  $D$ - waves

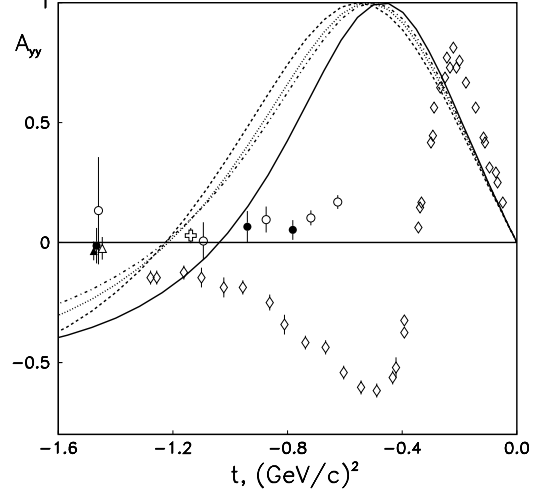


FIG. 6: Comparison of the tensor analyzing power  $A_{yy}$  in the  $(d, d')X$  reaction from the present experiment with the  $A_{yy}$  data in deuteron-proton elastic scattering at 3.43 GeV/c [21] (diamonds). The symbols for the  $(d, d')X$  reaction data and curves are the same as in Fig.4.

of the deuteron

$$\begin{aligned} T_{10} &= \frac{i}{\sqrt{2}} \int_0^\infty \left( u^2(r) - \frac{w^2(r)}{2} \right) j_0(rq/2)dr + \\ &+ \frac{i}{2} \int_0^\infty w(r) \left( u(r) + \frac{w(r)}{\sqrt{2}} \right) j_2(rq/2)dr. \end{aligned} \quad (7)$$

One can see that in the framework of the PWIA model [12], the vector analyzing power  $A_y$  is proportional to the ratio  $r$ , while the tensor analyzing power  $A_{yy}$  is defined mostly by the deuteron structure.

The curves shown in Fig.4 are the results of PWIA calculations [12] with different deuteron wave functions. The solid line is calculated with the deuteron wave function (DWF) for the Paris potential [19], while the dashed, dotted and dash-dotted lines correspond to the DWFs for Bonn A, B and C potentials [20], respectively.

The deviation of the data obtained in the previous experiments [1, 4] at  $|t| \sim 0.3-0.8$  (GeV/c)<sup>2</sup> from the predictions of PWIA, as well as from  $dp$ - [21] and  $ed$ - [22] elastic scattering, indicates the sensitivity of  $A_{yy}$  to the baryonic resonances excitation. In the framework of the multiple-scattering model, such a deviation may be due to a significant contribution of double-collision interactions corresponding to the diagrams shown in Figs.5b and 5c. The diagram of Fig.5b describes the situation, where the resonance is formed in the second  $NN$  collision whereas the resonance in the case of Fig.5c, formed in the first  $NN$  interaction, is then elastically scattered on the second nucleon of the deuteron. The calculations have shown that the contribution of the double-scattering terms is significant for  $|t|$  greater than  $\sim 0.4$  (GeV/c)<sup>2</sup> [23]. Therefore, in the framework of the

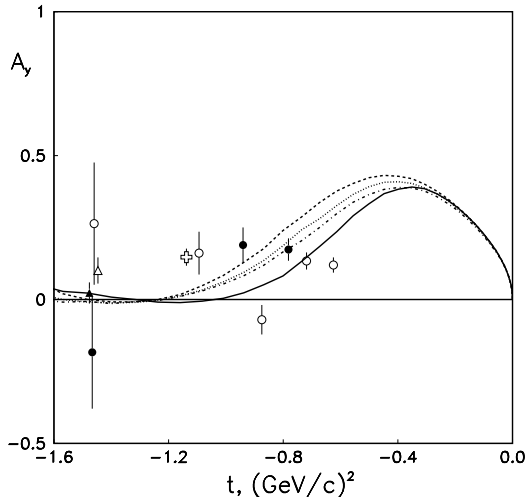


FIG. 7: Vector analyzing power  $A_y$  in the  $(d, d')X$  reaction from the present experiment compared with the PWIA predictions [12] using different DWFs.

multiple-scattering model, the behaviour of the tensor analyzing power  $A_{yy}$  is defined by the spin structure of the deuteron and the elementary amplitudes of the  $NN \rightarrow NN^*$  and  $NN^* \rightarrow NN^*$  processes.

The sensitivity of the tensor analyzing power in deuteron inelastic scattering off protons to the excitation of baryonic resonances is pointed out in the framework of the  $t$ -channel  $\omega$ -meson exchange model [10]. The diagram corresponding to this model is shown in Fig.5d. The cross section and polarization observables can be calculated from the known electromagnetic properties of the deuteron and baryonic resonances  $N^*$  through the vector dominance model. The details of the model are given in [10, 11]. This model satisfactorily explained the  $A_{yy}$  data in the  $(d, d')X$  reaction in the vicinity of low masses baryonic resonances [1, 2, 4]. In principle, this model can be applied for the explanation of the data of present experiment, however, the knowledge of the electromagnetic properties of the baryonic resonances with the masses 2.2–2.6 GeV/ $c^2$  is required.

Fig. 6 demonstrates the different behavior of the tensor analyzing powers in the  $(d, d')X$  process obtained in the present experiment and in  $dp$ - [21] elastic scattering, indicating different contribution of the double scattering at large  $|t|$ . One can see also, that the present  $A_{yy}$  data are in reasonable agreement with the PWIA prediction in the range of transferred 4-momentum  $|t|$  of 0.9–1.2 (GeV/ $c$ ) $^2$ .

The data on the vector analyzing power  $A_y$  obtained in the present experiment are plotted in Fig.7 versus  $t$ . The symbols corresponding to the data obtained in different kinematic conditions are the same as in Fig.4. It should be noted that the data obtained on hydrogen and carbon are in good agreement. The curves are obtained using the expression (4) with the ratio  $r$  of the spin-dependent

to spin-independent parts of the  $NN \rightarrow NN^*$  process taken in the form

$$r = a \cdot q \quad (8)$$

with the value of  $a = 0.4$  [12]. The solid curve in Fig.7 is obtained with the DWF for the Paris potential [19], while the dashed, dotted and dash-dotted lines correspond to the DWFs for Bonn A, B and C potentials [20], respectively. The PWIA calculations give approximately the same results at the value of  $a \sim 0.3$ –0.5. It should be noted that  $a$  might be different for different  $M_X$ , however, we took the fixed value for simplicity due to the lack of data. The observed relatively large value of  $A_y$  at  $|t| \sim 1$  (GeV/ $c$ ) $^2$  can be interpreted as being due to a significant role of the spin-dependent part of the elementary amplitude of the  $NN \rightarrow NN^*$  reaction.

#### IV. CONCLUSION

We have presented data on the tensor and vector analyzing powers  $A_{yy}$  and  $A_y$  in inelastic scattering  $(d, d')X$  of 9.0 GeV/ $c$  deuterons on hydrogen and carbon in the vicinity of the excitation of baryonic masses of  $\sim 2.2$ –2.6 GeV/ $c^2$ . This corresponds to the range of 4-momentum  $|t|$  between 0.7 and 2.5 (GeV/ $c$ ) $^2$ .

The data obtained on hydrogen and carbon targets are in good agreement. The observed independence of the analyzing powers on the atomic number of the target indicates that rescattering in the target and medium effects are small. Hence, nuclear targets are also appropriate to obtain information on the baryonic excitation in inelastic deuteron scattering [1]–[5].

The observed difference of the  $A_{yy}$  data at  $|t| \leq 0.8$  (GeV/ $c$ ) $^2$  with the PWIA calculations [12] using standard deuteron wave functions as well as with the data obtained in  $dp$ - [21] and  $ed$ -elastic scattering [22] indicates the sensitivity of  $A_{yy}$  to baryonic resonance excitation via double-collision interactions [23]. On the other hand, both  $A_{yy}$  and  $A_y$  data are in reasonable agreement with PWIA calculations [12] at  $|t| \sim 1$  (GeV/ $c$ ) $^2$ .

The large values of  $A_y$  show a significant role of the spin-dependent part of the elementary amplitude of the  $NN \rightarrow NN^*$  reaction in the vicinity of the baryonic masses excitation  $M_X \sim 2.2$  GeV/ $c^2$ .

#### Acknowledgments

Authors express their gratitude to Prof. A.I.Malakhov, Director of LHE, and Prof. V.N.Penev for their permanent help. Authors are grateful to the LHE accelerator staff and POLARIS team for providing good conditions for the experiment. They thank to L.V. Budkin, V.P. Ershov, V.V. Fimushkin, A.S. Nikiforov, Yu.K. Pilipenko, V.G. Perevozchikov, E.V. Ryzhov, A.I. Shirokov, and O.A. Titov for their assistance during the experiment.

Authors thank also A.N. Prokofiev and A.A. Zhdanov for the lending of the scintillation counters for the polarimeter. They are indebted to Prof. E.Tomasi-Gustafsson for

helpful discussions. This work was supported in part by the Russian Foundation for Basic Research under grants No. 03-02-16224 and No. 04-02-17107.

- 
- [1] L.S. Azhgirey et al., Phys. Lett. B **361**, 21 (1995).  
 [2] L.S. Azhgirey et al., JINR Rapid. Comm. N<sup>o</sup> **2[88]-98**, 17 (1998).  
 [3] L.S. Azhgirey et al., Yad. Fiz. **62**, 1796 (1999) [Phys. Atom. Nucl. **62**, 1673 (1999)].  
 [4] V.P. Ladygin et al., Eur. Phys. J. A **8**, 409 (2000); L.S. Azhgirey et al., Yad. Fiz. **64**, 2046 (2001) [Phys. Atom. Nucl. **64**, 1961 (2001)].  
 [5] L.S. Azhgirey et al., Yad. Fiz. **68**, 1029 (2005) [Phys. Atom. Nucl. **68**, 991 (2005)].  
 [6] Experiment LNS-E250 (unpublished)  
 [7] L.V. Malinina et al., Phys. Rev. C **64**, 064001 (2001).  
 [8] T. Suzuki, Nucl. Phys. A **577**, 167 (1994).  
 [9] Y. Satou et al., Phys. Lett. B **521**, 153 (2001).  
 [10] M.P. Rekaló and E. Tomasi-Gustafsson, Phys. Rev. C **54**, 3125 (1996).  
 [11] E. Tomasi-Gustafsson, M.P. Rekaló, R. Bijkeret al., Phys. Rev. C **59**, 1526 (1999).  
 [12] V.P.Ladygin and N.B.Ladygina, Yad. Fiz. **65**, 188 (2002) [Phys. Atom. Nucl. **65**, 182 (2002)].  
 [13] N.G. Anishchenko et al., in Proceedings of the 5-th International Symposium on High Energy Spin Physics (Brookhaven, 1982), AIP Conf.Proc. **95**, 445 (1983).  
 [14] L.S. Zolin et al., JINR Rapid. Comm. N<sup>o</sup> **2[88]-98**, 27 (1998).  
 [15] C.F. Perdrisat et al., Phys. Rev. Lett. **59**, 2840 (1987); V. Punjabi et al., Phys. Rev. C **39**, 608 (1989); V.G. Ableev et al., Pis'ma Zh. Eksp. Teor. Fiz. **47**, 558 (1988); V.G. Ableev et al., JINR Rapid Comm. N<sup>o</sup> **4[43]-90**, 5 (1990); T. Aono et al., Phys. Rev. Lett. **74**, 4997 (1995).  
 [16] V.P. Ladygin, Nucl. Instrum. Methods A **437**, 98 (1999).  
 [17] L.S. Azhgirey et al., Prib. Tekhn. Eksp. **1**, 57 (1997) [Instr. Exp. Tech. **40**, 43 (1997)].  
 [18] L.S. Azhgirey et al., Nucl. Instrum. Methods A **497**, 340 (2003).  
 [19] M. Lacombe et al., Phys. Lett. B **101**, 139 (1981).  
 [20] R. Machleidt et al., Phys. Rep. **149**, 1 (1987).  
 [21] M. Bleszynski et al., Phys. Lett. B **87**, 178 (1979); M. Haji-Saied et al., Phys. Rev. C **36**, 2010 (1987).  
 [22] M. Garçon et al., Phys. Rev. C **49**, 2516 (1994); D. Abbott et al., Phys. Rev. Lett. **84**, 5053 (2000); D.M. Nikolenko et al., Phys. Rev. Lett. **90**, 072501 (2003).  
 [23] L.S. Azhgirey et al., Yad. Fiz. **48**, 1758 (1988) [Sov. J. Nucl. Phys. **48**, 1058 (1988)].